Ther Adv Gastroenterol
2020, Vol. 13: 1–12
DOI: 10.1177/1756284820923220

Successful muscle regeneration by a homologous microperforated scaffold seeded with autologous mesenchymal stromal cells in a porcine esophageal substitution model

Maurizio Marzaro, Mattia Algeri, Luigi Tomao, Stefano Tedesco, Tamara Caldaro, Valerio Balassone, Anna Chiara Contini, Luciano Guerra, Giovanni Federici D'Abriola, Paola Francalanci, Maria Emiliana Caristo, Lorenzo Lupoi, Ivo Boskoski, Angela Bozza, Giuseppe Astori, Gianantonio Pozzato, Alessandro Pozzato, Guido Costamagna and Luigi Dall'Oglio

Correspondence to:
Ivo Boskoski
Fondazione Policlinico Universitario Agostino Gemelli IRCCS Largo A. Gemelli, 8, Rome 00168, Italy
ivo.boskoski@policlinicogemelli.it

Maurizio Marzaro
Pediatric Surgery Department, AULSS2 Treviso, Italy

Mattia Algeri
Luigi Tomao
Hemato-Oncology, Ospedale Pediatrico Bambino Gesù, Roma, Italy

Stefano Tedesco
Telea Biotech, Vicenza, Italy

Tamara Caldaro
Valerio Balassone
Anna Chiara Contini
Luciano Guerra
Giovanni Federici D'Abriola
Luigi Dall'Oglio
Digestive Endoscopy and Surgical Unit, Ospedale Pediatrico Bambino Gesù, Roma, Italy

Paola Francalanci
Pathology Department, Ospedale Pediatrico Bambino Gesù, Roma, Italy

Maria Emiliana Caristo
Lorenzo Lupoi
Università Cattolica del Sacro Cuore, Cen.Ri.S

Angela Bozza
Giuseppe Astori
LTCA, ULSS 8 Berica, Vicenza, Italy

Laboratorio di Terapie Cellulari Avanzate, Vicenza, Italy

Gianantonio Pozzato
Alessandro Pozzato
Telea Electronic Engineering, Vicenza, Italy

Guido Costamagna
Digestive Endoscopy Unit, Fondazione Policlinico Universitario Agostino Gemelli IRCCS, Rome, Italy

Abstract

Background: Since the esophagus has no redundancy, congenital and acquired esophageal diseases often require esophageal substitution, with complicated surgery and intestinal or gastric transposition. Peri-and-post-operative complications are frequent, with major problems related to the food transit and reflux. During the last years tissue engineering products became an interesting therapeutic alternative for esophageal replacement, since they could mimic the organ structure and potentially help to restore the native functions and physiology. The use of acellular matrices pre-seeded with cells showed promising results for esophageal replacement approaches, but cell homing and adhesion to the scaffold remain an important issue and were investigated.

Methods: A porcine esophageal substitute constituted of a decellularized scaffold seeded with autologous bone marrow-derived mesenchymal stromal cells (BM-MSCs) was developed. In order to improve cell seeding and distribution throughout the scaffolds, they were micro-perforated by Quantum Molecular Resonance (QMR) technology (Telea Electronic Engineering).

Results: The treatment created a microporous network and cells were able to colonize both outer and inner layers of the scaffolds. Non seeded (NSS) and BM-MSCs seeded scaffolds (SS) were implanted on the thoracic esophagus of 4 and 8 pigs respectively, substituting only the muscle layer in a mucosal sparing technique. After 3 months from surgery, we observed an esophageal substenosis in 2/4 NSS pigs and in 6/8 SS pigs and a non-practicable stricture in 1/4 NSS pigs and 2/8 SS pigs. All the animals exhibited a normal weight increase, except one case in the SS group. Actin and desmin staining of the post-implant scaffolds evidenced the regeneration of a muscular layer from one anastomosis to another in the SS group but not in the NSS one.

Conclusions: A muscle esophageal substitute starting from a porcine scaffold was developed and it was fully repopulated by BM-MSCs after seeding. The substitute was able to recapitulate in shape and function the original esophageal muscle layer.

Keywords: 3D cell culture, esophagus, mesenchymal stromal cells, Quantum Molecular Resonance, scaffold, tissue engineering

Received: 8 November 2019; revised manuscript accepted: 6 April 2020.

Introduction

Esophageal reconstruction consists of complicated surgery with gastric or intestinal transpositions, with significant morbidity and post-operative long-term complications resulting in a poor quality of life for patients.[1–5] Moreover, since the esophagus has no redundancy, only a limited number of esophageal resections can be performed with successful termino-terminal anastomosis.[6,7]

Tissue-engineering (TE) products recently raised much interest as an alternative for esophageal replacement.[8] They could allow creation of tailored esophageal substitutes, which could promote an *in vivo* regeneration of particular interest in the pediatric age, since they could follow host growth and reduce surgical complications.

Different techniques and several experimental trials have been described in animals for TE esophageal repair,[9,10] but results are difficult to compare due to the different animal models used (rat, rabbit, dog, minipig, pig), the timing of the autopsy (from a few weeks to several months), the targeted area (mucosa, muscular wall), the dimensions and location of the esophageal defect and the materials used as scaffold (natural or synthetic).[9,11–14] Decellularized scaffolds are consequently more suitable for this application[9,15] since the extracellular matrix (ECM) components are actively involved in cell adhesion, growth, proliferation and differentiation, and they better mimic the original tissue architecture and function.[10,16–19] However, their three-dimensional (3D) dense structure, due to the high protein content and the tight matrix structure, represents itself a limit for an optimal cell seeding inside and an issue to overcome to obtain the full cell repopulation in the inner parts of the scaffold.[13,16]

Acellular scaffolds implanted alone allow repopulation by host cells when used for small defects, whereas when longer reconstruction is required, the scaffold alone leads to poor remodeling and to stricture formation.[20–24] Instead, cell-seeded scaffolds reduce inflammation and increase regeneration.[12,25–27] Among the different cell types tested in combination with biomaterials,[9] the mesenchymal stromal cells (MSCs) gained particular interest for esophageal regenerative approaches due to their ability to differentiate into mesodermal tissues. They are multipotent progenitor cells, and show the ability to differentiate *in vitro* into osteocytes, chondrocytes and adipocytes,[28,29] and are mainly used for their immunomodulatory properties[30–34] basing on their cytokines[35] and exosome[36] secretion that have anti-inflammatory, chemoattractive and proangiogenic properties.[31,37–40] When used in combination with acellular matrix for esophageal replacement strategies, MSCs were shown to promote re-epithelialization, to accelerate muscle colonization and regeneration, and to exert an anti-inflammatory role.[41–44]

In this study, we describe a preliminary approach to the esophageal substitution based on a homologous decellularized scaffold[45,46] seeded with autologous bone-marrow-derived MSCs (BM-MSCs). In order to enhance cell seeding throughout the scaffold, this was microperforated by needles using Quantum Molecular Resonance® (QMR).[45,46] This technology creates quanta of energy able to break the molecular bonds at the tip of the needles without increasing the kinetic energy of the hit molecules; thus, without raising temperature, thus limiting the damage to the surrounding tissue.[47]

Materials and methods animals

Experiments involving animals were performed in compliance with directive 2010/63/EU on the protection of animals used for scientific purposes and in compliance with the Italian animal welfare and veterinary health rules and regulations concerning the care and utilization of laboratory animals (authorization 786/2016-PR, 8.08.2016). For this study, 12 pigs (*Sus scrofa domesticus*) have been used.

Esophagus collection

The esophagi were obtained from seven donor pigs weighing about 40 kg, and two adequate scaffolds were obtained from each donor.

Animals were kept fastened for 12 h before surgery, with water diet and glucose solution until midnight before the operation. They received antibiotic therapy with ceftiofur (Excenel, Zoetis Italia Srl, Roma, Italy) 3 mg/kg/day, administered intramuscularly at 1 ml/16 kg for each injection. The administration started 24 h before the operation. A venous catheter was placed in the auricular vein. Anesthesia was induced with diazepam 0.5 mg/kg and ketamine 1–5 mg/kg or alternatively propofol 1–8 mg/kg, and was maintained through 2–3% isoflurane and continuous infusion of propofol (2 mg/kg). Muscle relaxation was obtained by continuous infusion of

Tracrium® (atracurium, Glaxosmithkline Spa, Via Alessandro Fleming, Verona, Italy) 1 mg/kg. Intubation was performed using 4/5.5 mm cuffed tracheotubes and the animals were kept in mechanical ventilation during the entire operation, blood pressure and blood parameters were monitored, and 5% glucose, crystalloids and colloids were administered if necessary.

With the animal in a left lateral decubitus, the esophagus was reached and removed through a right thoracotomy. The cervical and cardiac portions were removed to get rid of the mixed muscular layer and the resulting thoracic esophagus was rinsed twice in ultra-pure water and then stored in a solution containing ultra-pure water and 2% penicillin/streptomycin (10^4 U/ml penicillin and 10 mg/ml streptomycin in 0.9% NaCl; AF).

At the end of the procedure, animals were sacrificed by endovenous injection of Tanax® (MI, Italy) 3 ml/10 kg.

Esophagus decellularization

Samples were cut longitudinally, and the *tunica mucosa* and submucosa were removed, leaving the muscular layer only. They were then washed in ultra-pure water and 2% AF for 48 h at 4°C in static conditions and incubated five times for 4 h at room temperature in 4% sodium deoxycholate (BioXtra ⩾98.0%, Sigma-Aldrich, now Merck KGaA, Darmstadt, Germany). Samples were then treated five times with 2000 KU of DNase-I (Warthington, NJ, USA) in 1 mmol/l NaCl for 3 h at room temperature and then rinsed four times in ultra-pure water. In order to remove decellularization reagents, samples were washed with increasing percentages of denatured ethanol (ACS reagent (NJ, USA), ⩾99.8%, without additive, Honeywell) and then rehydrated in ultra-pure water. Scaffolds were then stored in ultra-pure water and 2% AF at 4°C.

DNA extraction and quantification

Efficiency of the decellularization protocol was evaluated by deoxyribonucleic acid (DNA) quantification. Double-stranded DNA was quantified both in decellularized and control tissue samples. DNA was isolated using the DNeasy Blood and Tissue kit (Qiagen, Hilden, Germany) following manufacturer's instructions. Briefly, a maximum of 25 mg tissue was cut into small pieces and digested overnight at 56°C with Proteinase K in buffer ATL. After addition of ethanol and buffer ATL, samples were transferred into spin columns and centrifuged for 1 min at 8000 rpm. After two washing steps with Buffer AW1 (8000 rpm for 1 min) and AW2 (14,000 rpm for 3 min), DNA was eluted by incubation for 1 min with Buffer AE and centrifugation at 8000 rpm for 1 min. DNA was quantified by using a BioPhotometer Plus (Eppendorf, Barkhausenweg, Hamburg, Germany). Optical densities at 260 nm and 280 nm were used to estimate the purity and yield of DNA (Kit for residual DNA quantification: DNeasy Blood & Tissue Kit (50), Qiagen Cat No./ID: 69504).

Scaffold QMR perforative treatment

For the purpose of increasing the number of cells to be seeded and to improve their diffusion, the scaffolds were subjected to a patented microscopic perforative treatment (Telea Biotech, subsidiary of Telea Electronic Engineering, Sandrigo VI, Italy). We used a 150 μm diameter needle mounted on a three-axis Cartesian robot handpiece (Yamaha model RCX240, Hamamatsu, Shizuoka, Japan) that performed a regular perforation of the scaffold through a dedicated algorithm. The needle was connected to the VESALIUS® current generator that uses QMR technology. Since this particular current works below 50°C, it has been documented to avoid burns or any degeneration of connective tissue.[45,46,48,49] Once used in our procedure, it allows the creation of channels inside the scaffold while preserving all the natural scaffold characteristics. The perforation procedure was extended to the entire scaffold thickness and surface and was performed in a class II biological safety cabinet under aseptic conditions. The creation of pores and their dimensions were analyzed with digital microscope (Vision Engineering model EVO Cam, MI, Italy) and with scanning electron microscopy at different magnifications and are reported hereafter.

BM-MSCs isolation and expansion

An amount of 10 ml BM was collected from the femur of animals who were candidates for esophageal substitution, under sedation and local anesthesia. Mononuclear cells were isolated by density-gradient centrifugation ($d = 1.077$ g/ml; Lympholyte, Cedarlane Laboratories) and plated in non-coated tissue culture flasks at a density of 1.6×10^5 cells/cm^2 in complete culture medium

consisting of Dulbecco's modified eagles' medium (DMEM; Euroclone, Pero, Italy) supplemented with 10% fetal bovine serum (FBS; Life Technologies, now Thermo Fisher Scientific, MA, USA), 50 U/ml penicillin, 50 mg/ml streptomycin and 2 mmol/l L-glutamine (Euroclone). Cultures were maintained at 37°C in a 5% CO_2 incubator. After 48 h, non-adherent cells were removed, and culture medium was replaced twice weekly. At 80% confluence, BM-MSCs were detached with Trypsin-EDTA (Euroclone) and expanded at 4×10^3 cells/cm^2 density.

MSCs phenotypical characterization

BM-MSCs were phenotypically characterized by flow cytometry (FACS-Canto, Becton Dickinson) with different fluorophore-conjugated monoclonal antibodies specific for porcine CD14, CD29, CD44 and CD45 (BD PharMingen, New Jersey, USA). Isotype antibodies were used as negative controls. Data were analyzed using FACSDiva software (Tree Star, software produced by BD Biosciences, New Jersey, USA).

BM-MSCs adipogenic and osteogenic differentiation

Differentiation protocols were performed with BM-MSCs at P2, as previously described.[50] Cells were cultured in minimum essential medium eagle–alpha modification (αMEM, Euroclone) supplemented with 10% FBS, 2 mmol/l L-glutamine, 50 U/ml penicillin, 50 mg/ml streptomycin, 10−7 mol/l dexamethasone and 50 mg/ml L- ascorbic acid. For osteogenic differentiation, 5 mmol/l ß-glycerol phosphate (Sigma-Aldrich) was added to the culture medium from day 7, whereas for adipogenic differentiation, 100 mg/ml insulin, 50 mmol/l isobutyl methylxanthine, 0.5 mmol/l indomethacin (Sigma-Aldrich), and 5 mmol/l β-glycerol phosphate were added to the culture medium. Cultures were incubated for at least 2 weeks before analyzing cell differentiation.

Osteogenic differentiation was analyzed by staining of alkaline phosphatase (AP) activity with Fast Blue and calcium deposition with Alizarin Red and quantification at 550 nm. Adipogenic differentiation was evaluated by Oil Red O extraction and quantification at 550 nm. DNA was extracted from each sample and the amount of released Oil Red O and AP was normalized to the relative DNA content.

BM-MSCs seeding on decellularized scaffolds

Decellularized scaffolds 4 cm in length were incubated for 2 h with 5 ml cell suspension (1×10^6 cells/ml) in a 100 mm petri dish. Then, 20 ml complete medium was added and scaffolds were incubated for 10 days prior to implantation. Medium was changed daily.

Esophagus implantation

Animals were prepared for surgery and anesthetized as previously described. Anesthesia was maintained through isoflurane 1.3–3% administration by inhalation. Intra-operative analgesia was obtained by fentanyl 2–20 μg/kg/h (intravenously, IV), antibiotic coverage was guaranteed by cefazolin 25 mg/kg (IV) and omeprazole 0.7–1 mg/kg (IV) was administered at the same time.

The recipient pigs had a right thoracotomy, the posterior mediastinum was reached through the extra-pleural route and the thoracic esophagus exposed, as in esophageal atresia repair during neonatal surgery. A cylinder of the muscular layer only was removed of 4 cm length, leaving intact the mucosa, and the seeded scaffold was used as a sheet to cover the gap of the surrounding the mucosa. For this purpose, we used two termino-terminal (T-T) anastomoses, upper and lower, with the native muscular layer, and one longitudinal anastomosis to close the scaffold on itself with 6.0 running sutures. No pedicled omental flap was used to increase the scaffold vascularization, no thoracic drainage was used, and no stent was positioned to open the esophageal lumen.

This technique represents a preliminary approach to the full-thickness TE esophageal-wall substitution. Our purpose was to test the ability of the microperforated scaffold to keep the MSC cultures inside, realizing a 3D cell culture and to verify its regenerative properties once using the vascular potential of the anastomosis. For this purpose we chose a planar scaffold based only on the homologous muscular esophageal wall. Once implanted, it resembled the normal anatomical layout of the native esophagus muscular layer and allowed us to study the scaffold properties in revascularization and muscular regeneration.

Four animals were implanted with non-seeded scaffolds (NSS); eight with seeded scaffolds (SS). In the NSS group, an esophageal cylindrical patch with an average size of 3.9 × 3.6 cm (minimum 3.5 × 3.2 cm,

maximum 4.5 × 3.6 cm) was implanted. In one case, the patch was 1.3 × 3 cm in size.

Post-operative evaluation and follow-up

Post-operative analgesia was maintained with tramadol 5 mg/kg and ketorolac 1 mg/kg intramuscularly for at least 4/5 days, according to veterinarian evaluation. As soon as possible, glucose solutions and liquid diet were administered to the animals, followed by a standard diet.

A regular follow-up with esophageal barium meal and endoscopy was performed after 15 days, 1 and 2 months from surgery. Animals were also daily controlled for behavior, food intake, regurgitation, vomiting, dysphagia and weekly weighed. They were sacrificed after 3 months from surgery and autopsies were performed. The esophagi were removed from the animals, implanted scaffolds were retrieved, and two specimens of each implant were collected for further analyses, one at the anastomotic site and one from the scaffold itself.

Histology and immunohistochemistry

Samples were snap-frozen or fixed in formalin. Sections of 3 mm were stained with haematoxylin-eosin (HE) and with Masson's trichrome for evaluating decellularization efficiency in pre-implanted scaffolds and visualizing muscle and connective components in retrieved scaffolds. Analysis of the muscular components was done through immunohistochemistry with anti-actin (ready to use, Dako, Glostrup Municipality, Denmark) and anti-desmin (ready to use, Dako, Glostrup Municipality, Denmark) antibodies with subsequent streptavidin–biotin–peroxidase staining. Sections were visualized by 3,3′-diaminobenzidine (DAB) and counterstained with hematoxylin. Images were obtained with Olympus BX53.

Statistical analysis

Quantitative data are presented as mean ± standard deviation. Non-random associations between categorical variables was calculated by using the Fisher's exact test (p value).

Results

Esophagus decellularization

Decellularized esophagi appeared translucent [Figure 1(a)] compared with non-treated ones [Figure 1(b)]. Decellularization efficiency was evaluated comparing DNA quantification in decellularized dry tissues and five esophagi obtained from non-stabularized pigs. Moreover, in order to evaluate decellularization efficiency along the whole length of the esophagus, each scaffold was divided into two portions, the cervical one and the cardiac one, and DNA quantified. Table 1 shows that in all decellularized scaffolds DNA content was under 50 ng/mg threshold and significantly lower with respect to non-treated fresh esophagi, demonstrating an efficient decellularization in all samples. Moreover, average DNA content in cervical and cardiac portions (Table 1) confirm the efficiency of the treatment throughout the scaffolds, with no significant differences among cervical and cardiac portions of the same sample (Table 2). A DNA value <50 ng/mg ECM tissue is considered the optimal assessment.[51] DNA extraction and quantification is intended on dry tissue.

Table 1. Average DNA content and relative standard deviation on fresh and decellularized esophagi. Average DNA content for decellularized samples was calculated considering both cervical and cardial portions. Values are expressed in ng/mg ECM tissue.

	Average DNA content (ng DNA/mg ECM tissue)	Standard deviation
Fresh esophagi	346.65	±129.02
Decellularized esophagi	34.84	±13.33
Cervical portions	34.25	±12.97
Cardiac portions	35.29	±12.29

DNA, deoxyribonucleic acid; ECM, extracellular matrix.

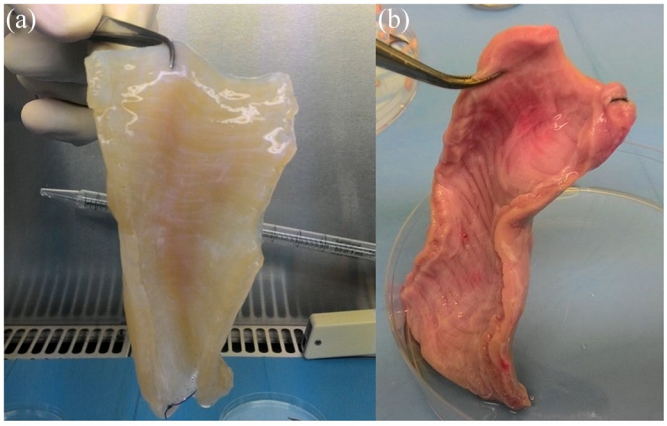

Figure 1. The appearance of esophagi.
(a) Decellularized esophagus; (b) fresh esophagus.

Table 2. DNA content on cervical and cardial portions of each acellular esophagus analyzed. Values are expressed in ng/mg ECM tissue.

Average DNA content (ng DNA/mg ECM tissue)		
Sample	**Cervical portion**	**Cardiac portion**
Pig 1	17.00	17.60
Pig 2	33.50	37.50
Pig 3	49.05	47.65
Pig 4	48.80	48.70
Pig 5	23.64	25.00

DNA, deoxyribonucleic acid; ECM, extracellular matrix.

Scaffold perforative treatment

After the QMR perforative treatment [Figure 2(a)] the scaffold showed no burns or connective tissue damages [Figure 2(b)]. The scaffold dimensions and thickness appeared preserved as well as the ECM architecture [Figure 2(b, c)].

The QMR treatment realized about 1200 pores/cm^2 in a regular distribution throughout the scaffold [Figure 2(d)], each pore having a diameter ranging from 80 to 100 µm and a similar interspace [Figure 2 (e, f)].

BM-MSC isolation and characterization

MSCs were successfully derived from BM samples. The obtained cells displayed the characteristic spindle-shaped morphology of MSCs [Figure S1(a)] and flow cytometry analyses showed specific MSC-marker expression (CD29 and CD44) and lack of hematopoietic markers (CD14 and CD45) [Figure S1(d, e)]. BM-MSCs were able to differentiate both into osteoblasts [Figure S1(b)] and adipocytes [Figure S1(c)].

BM-MSC seeding in static condition

Decellularized scaffolds were incubated with BM-MSCs. Cells successfully adhered to the surface of the scaffold at the end of the incubation period, also colonizing channels and pores, as shown by scanning electron microscopy (SEM) images where adherent cells are visible in scaffold inner walls [Figure 3(a, b)].

Scaffold implantation and animal follow-up

The average weight of animals at the time of surgery was 38.6 kg (minimum 30 kg, maximum 46 kg) and the surgical procedures lasted 217 min, on average (minimum 135 min, maximum 315 min). The implanted scaffolds covered the mucosa through two T-T and one longitudinal anastomosis

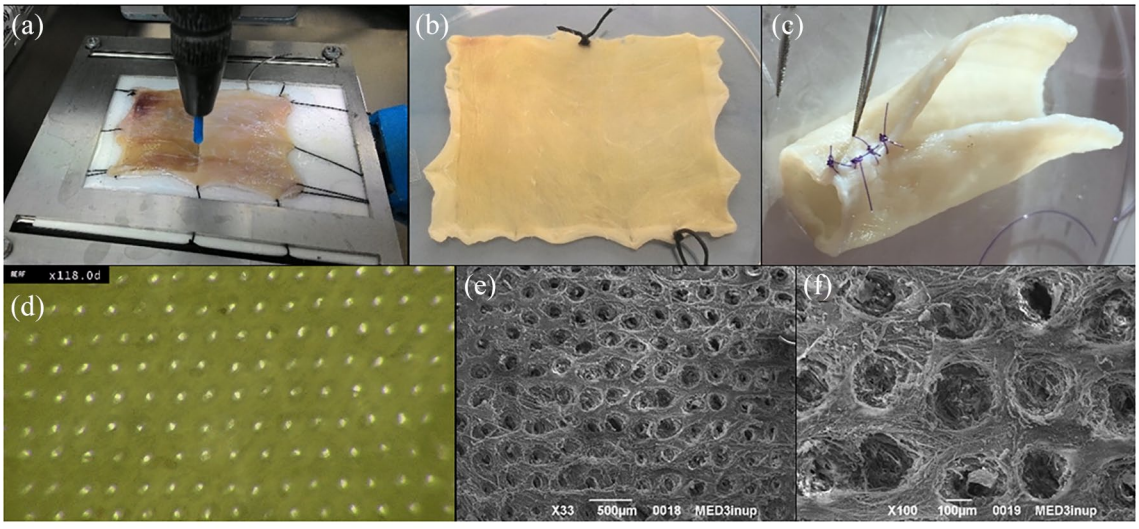

Figure 2. Scaffold perforative treatment.
(a) Perforative QMR procedure with the needle connected to a Cartesian robot; (b) macroscopic scaffold appearance after QMR perforative treatment in rectangular open shape; (c) macroscopic scaffold appearance after QMR perforative treatment in tubular shape; (d) digital microscope image of the upper surface of a decellularized scaffold after QMR perforative treatment at 118× magnification; (e) SEM image of a decellularized scaffold after QMR perforative treatment, magnification: 33×, scale bar 100 µm; (f) SEM image of a decellularized scaffold after QMR perforative treatment, magnification: 100×, scale bar 100 µm.
QMR, Quantum Molecular Resonance®; SEM, scanning electron microscopy.

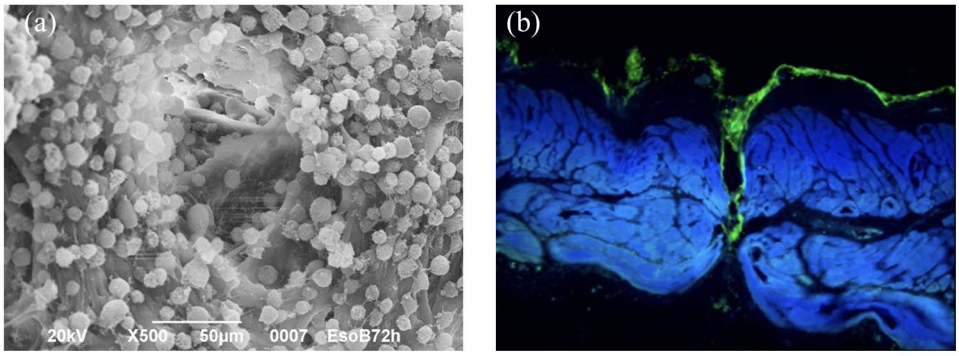

Figure 3. SEM image of a decellularized scaffold seeded with MSCs and cell culture outside and inside channels.
(a) SEM image of a decellularized scaffold seeded with MSCs: magnification 500×, scale bar 50 µm; (b) cell culture (actina marchers) outside and inside channels.
MSC, mesenchymal stromal cell; SEM, scanning electron microscopy.

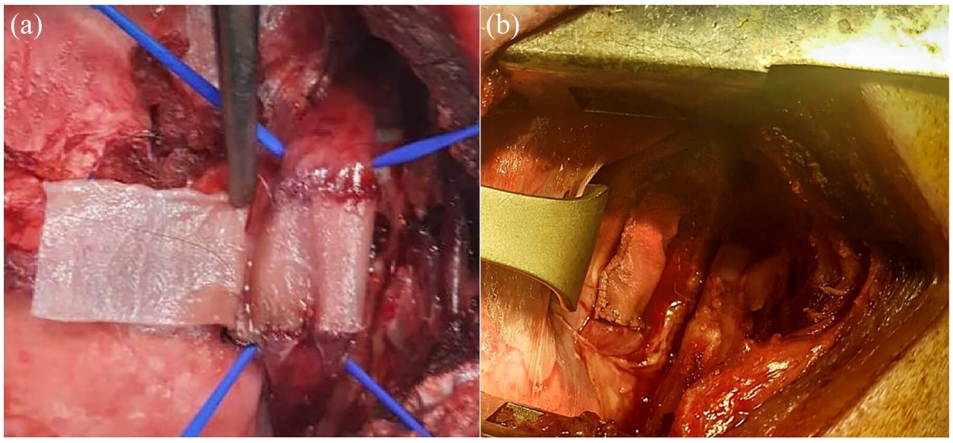

Figure 4. Scaffold implantation.
(a) Image of surgical procedure with a decellularized scaffold during implantation, with the scaffold wrapping around the esophagus mucosa in a tubular shape with two T-T and one longitudinal anastomosis; (b) image of the decellularized scaffold at the end of surgical procedure.
T-T, termino-terminal.

(Figure 4). One animal presented with bradycardia and hyperthermia, solved through the IV administration of adrenaline and steroids, together with ventilatory support. All the animals survived the procedure.

In the post-operative period, all the animals started to feed normally, since the mucosal layer was left intact during surgery. Radiology showed an esophageal relative stenosis in 50% (2/4) of NSS pigs and in 75% (6/8) of SS pigs; however, this difference was not statistically significant ($p = 0.5475$). A non-practicable stricture to the 11 mm diameter endoscope was observed in 25% (1/4) of NSS pigs and in 25% (2/8) of SS pigs ($p > 0.9999$). Therefore, the SS implant did not cause a significant increase in the incidence of esophageal stenosis compared with the NSS one. All animals showed normal weight increase, behaved normally, and did not suffer from pain. Stenosis at the surgical site caused a reduced food intake only in one animal of the SS group, with progressive weight loss, and the animal was euthanized at 2 months post-surgery.

Histology

Histological analyses on post-implant scaffolds showed vascularized fibrous tissue without muscular component in the NSS group, demonstrated

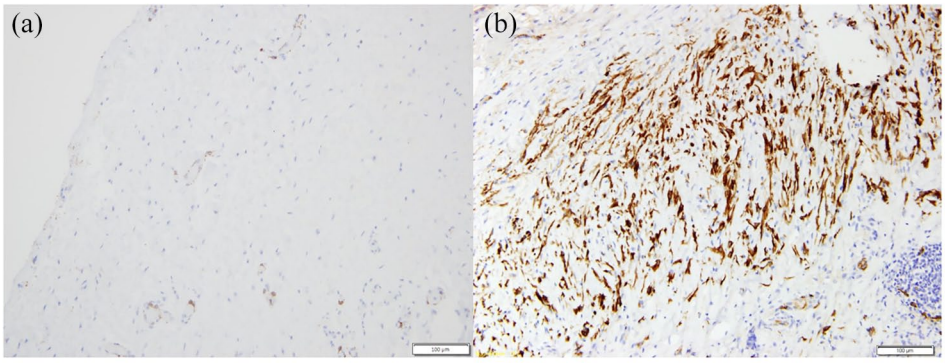

Figure 5. Histological analyses.
(a) NSS retrieved after 3 months from surgery, desmin staining, magnification: 20×; (b) SS scaffold retrieved after 3 months from surgery, actin and desmin staining, magnification: 20×.
NSS, non-seeded scaffold; SS, seeded scaffold.

by the negativity to desmin and actin staining [Figure 5(a)].

In all scaffolds retrieved from the SS group, we observed an inflammatory tissue evidenced by mononucleated cells and neo vessels. However, we observed also the presence of actin- and desmin-positive cells [Figure 5(b)] organized in a neo-muscular layer throughout the whole scaffold, indicating that muscle regeneration occurred.

Discussion

Tissue-engineered scaffolds are gaining great interest for esophageal regeneration since intestinal or gastric transpositions for the treatment of esophageal congenital or acquired defects are highly invasive procedures, often resulting in post-operative complications and poor quality of life.[14] Synthetic non-absorbable materials such as Teflon®, polyethylene terephthalate, expanded polytetrafluoroethylene, or silicone were tested as esophageal substitutes, showing poor biocompatibility, chronic infections, anastomotic leakage, material extrusion, and strictures.[9,11,14,52,53] Acellular natural biomaterials instead are considered promising scaffold, as they better resemble tissue-original architecture and structure, allow vascular ingrowth, do not release toxic degradation products, contain ECM components, which are important for several cellular functions and already show higher biocompatibility and biodegradability when used as esophageal substitutes.[9,14,53] It has also been shown that the host response to implanted xenogeneic or allogeneic bioscaffolds is similar, due to similarity among mammalian ECM components;[54] therefore, increasing the hope that human organs with low regenerative potential, such as the esophagus, could be substituted with animal-derived tissues. Moreover, the first studies have been published on the use of acellular commercial materials, both from human and animal origins, in human patients requiring esophageal replacement, and they report promising results.[53,55–59]

In animal models, the use of pre-SS for full-circumferential esophageal reconstruction resulted in a higher degree of regeneration and lower inflammation rates with respect to scaffold implanted alone.[12,25–27,44] We also reported that the use of a homologous esophageal decellularized scaffold seeded with muscle cells for partial muscular substitution of the esophageal wall resulted in better outcomes with respect to counterparts without cells. Our previous results demonstrated the development of an inner muscular layer growing synchronously with the animals, avoiding stenosis and dysphagia in SS but not in scaffolds alone. The study confirmed efficacy of the approach, despite the partial tissue regeneration, due to the limited amount of cells efficiently seeded on the scaffold.[12] This is why we made the choice of the QMR perforative treatment of the decellularized homologous esophageal scaffold in order to increase the number of the seeded cells. SEM images showed that QMR treatment creates a micropore network in the matrix and that, once seeded with MSCs and incubated for 10 days, cells were present and adhered both to the outer surface and to the inner part of the scaffold. Some studies tested the combination of natural and synthetic biomaterials in order to enhance cell adhesion and cell–scaffold

interactions,[44] however, increasing the complexity of the scaffolds.

The scaffolds we used in this trial derive from homologous esophagi after removal of mucosal and submucosal layers. A group of animals was implanted with scaffolds alone (NSS) and another group with scaffolds seeded with MSCs (SS). As a preliminary approach to the esophageal replacement, we substituted only the muscular layer of the native esophagus, leaving intact the mucosa, thus allowing the animals to resume oral feeding immediately after surgery, in the attempt to study the regenerative possibilities of such a scaffold. The surgical model we used was safe and feasible, since it mimics the surgical approach and the operative field of an in-human setting, allowing performance of a full trial without considerable complications and leaving the animals to a normal oral feeding for all the experimental period.

After 3 months from surgery, we analyzed the expression of desmin, an intermediate filament protein considered an indicator of active muscle-cell differentiation,[60] both in the scaffold and at the anastomotic regions. No desmin-positive cells were detected in animals implanted with NSS. On the contrary, all the animals implanted with SS showed the presence of desmin-positive cells, indicating that muscle regeneration occurred in this group, with muscle ingrowth inside the scaffold connective tissue from one anastomosis to the other one. These data confirm the efficacy of using pre-SS with respect to scaffolds alone, as previously reported in our work and by others.[12,25–27] We did not investigate whether regenerating muscle cells present in SS group were differentiated MSCs or muscle cells that migrated from the anastomoses to the site of the implant. In fact, MSCs are known to be able to differentiate into muscle cells and also to have immunomodulatory and regenerative properties.[31,32,38–40] This would be investigated in future studies in which we would also evaluate the biocompatibility of our scaffolds and regeneration rates with longer follow-up. This study focused on the regeneration of the muscle layer alone and allowed the optimization of the biological and surgical model. However, as the esophagus is a complex organ composed of different layers, we are planning further studies to develop an esophageal substitute able to replicate all the native-layered structure of the esophagus.

Conclusion

We developed a homologous acellular esophageal scaffold valuable for esophageal replacement approaches. QMR perforative treatment of the scaffold resulted in a multiporous network that allowed an efficient colonization with cells of both outer surface and inner parts of the scaffold without damaging its dimensions and architecture. After the implantation in a large animal model, we confirmed better outcomes obtained with pre-SS, evidenced by muscle regeneration. QMR could therefore be considered a promising technology for enhancing cell adhesion and full colonization of natural scaffolds, increasing the TE substitutes regenerative potential.

This trial represents a preliminary approach to an esophageal reconstruction procedure. These promising results are the base for planning a full thoracic esophageal substitution involving a tubular microperforated decellularized scaffold derived from a whole-donor esophagus.

Author contributions

Conceptualization and study design: MM, LDO, MEC, GC. Laboratory experiments: MM, ST, AB, LT, MA, PF, GP. Animal surgery: LDO, LL, IB, MM, TC, VB, ACIC, LG, GFD, MEC. Data interpretation: LDO, MM. Manuscript writing, reviewing, and editing: MM, AB, GA. All authors read and approved the final manuscript.

Funding

The authors disclose receipt of the following financial support for the research, authorship, and/or publication of this article: the work has been supported by Telea Biotech and by the Italian Ministry of Health within the Ricerca Corrente 2017 Program of the Bambino Gesù Children's Hospital.

Conflict of interest statement

GC is a consultant for Olympus, Cook Medical, and Boston Scientific. IB is a research grant holder from Apollo Endosurgery and a consultant for Apollo Endosurgery, Cook Medical, and Boston Scientific.

ORCID iD

Boskoski, Ivo https://orcid.org/0000-0001-8194-2670

Supplemental material

Supplemental material for this article is available online.

References

1. Ludman L and Spitz L. Quality of life after gastric transposition for oesophageal atresia. *J Pediatr Surg* 2003; 38: 53–57.
2. Ure BM, Slany E, Eypasch EP, *et al.* Long- term functional results and quality of life after colon interposition for long-gap oesophageal atresia. *Eur J Pediatr Surg* 1995; 5: 206–210.
3. Awad K and Jaffray B. Oesophageal replacement with stomach: a personal series and review of published experience. *J Paediatr Child Health* 2017; 53: 1159–1166.
4. Swisher SG, Deford L, Merriman KW, *et al.* Effect of operative volume on morbidity, mortality, and hospital use after esophagectomy for cancer. *J Thorac Cardiovasc Surg* 2000; 119: 1126–1132.
5. Sauvanet A, Mariette C, Thomas P, *et al.* Mortality and morbidity after resection for adenocarcinoma of the gastroesophageal junction: predictive factors. *J Am Coll Surg* 2005; 201: 253–262.
6. Meezan E, Hjelle JT, Brendel K, *et al.* A simple, versatile, nondisruptive method for the isolation of morphologically and chemically pure basement membranes from several tissues. *Life Sci* 1975; 17: 1721–1732.
7. Gawad KA, Hosch SB, Bumann D, *et al.* How important is the route of reconstruction after esophagectomy: a prospective randomized study. *Am J Gastroenterol* 1999; 94: 1490–1496.
8. Orlando G, Soker S and Stratta RJ. Organ bioengineering and regeneration as the new holy grail for organ transplantation. *Ann Surg* 2013; 258: 221–232.
9. Arakelian L, Kanai N, Dua K, *et al.* Esophageal tissue engineering: from bench to bedside. *Ann N Y Acad Sci* 2018; 1434: 156–163.
10. Londono R and Badylak SF. Regenerative medicine strategies for esophageal repair. *Tissue Eng Part B Rev* 2015; 21: 393–410.
11. Poghosyan T, Catry J, Luong-Nguyen M, *et al.* Esophageal tissue engineering: current status and perspectives. *J Visc Surg* 2016; 153: 21–29.
12. Marzaro M, Vigolo S, Oselladore B, *et al.* In vitro and in vivo proposal of an artificial esophagus. *J Biomed Mater Res A* 2006; 77: 795–801.
13. Luc G, Charles G, Gronnier C, *et al.* Decellularized and matured esophageal scaffold for circumferential esophagus replacement: proof of concept in a pig model. *Biomaterials* 2018; 175: 1–18.
14. Totonelli G, Maghsoudlou P, Fishman JM, *et al.* Esophageal tissue engineering: a new approach for esophageal replacement. *World J Gastroenterol* 2012; 18: 6900–6907.
15. Beckstead BL, Pan S, Bhrany AD, *et al.* Esophageal epithelial cell interaction with synthetic and natural scaffolds for tissue engineering. *Biomaterials* 2005; 26: 6217–6228.
16. Badylak SF, Freytes DO and Gilbert TW. Extracellular matrix as a biological scaffold material: structure and function. *Acta Biomaterialia* 2009; 5: 1–13.
17. Vorotnikova E, McIntosh D, Dewilde A, *et al.* Extracellular matrix-derived products modulate endothelial and progenitor cell migration and proliferation in vitro and stimulate regenerative healing in vivo. *Matrix Biology* 2010; 29: 690–700.
18. Langer R and Tirrell DA. Designing materials for biology and medicine. *Nature* 2004; 428: 487–492.
19. Londono R and Badylak SF. Biologic scaffolds for regenerative medicine: mechanisms of in vivo remodeling. *Ann Biomed Eng* 2015; 43: 577–592.
20. Doede T, Bondartschuk M, Joerck C, *et al.* Unsuccessful alloplastic esophageal replacement with porcine small intestinal submucosa. *Artif Organs* 2009; 33: 328–333.
21. Totonelli G, Maghsoudlou P, Georgiades F, *et al.* Detergent enzymatic treatment for the development of a natural acellular matrix for oesophageal regeneration. *Pediatr Surg Int* 2013; 29: 87–95.
22. Badylak S, Meurling S, Chen M, *et al.* Resorbable bioscaffold for esophageal repair in a dog model. *J Pediatr Surg* 2000; 35: 1097–1103.
23. Urita Y, Komuro H, Chen G, *et al.* Regeneration of the esophagus using gastric acellular matrix: an experimental study in a rat model. *Pediatr Surg Int* 2007; 23: 21–26.
24. Lopes MF, Cabrita A, Ilharco J, *et al.* Esophageal replacement in rat using porcine intestinal submucosa as a patch or a tube- shaped graft. *Dis Esophagus* 2006; 19: 254–259.
25. Badylak SF, Vorp DA, Spievack AR, *et al.* Esophageal reconstruction with ECM and muscle

tissue in a dog model. *J Surg Res* 2005; 128: 87–97.

26. Marzaro M, Conconi MT, Perin L, *et al.* Autologous satellite cell seeding improves in vivo biocompatibility of homologous muscle acellular matrix implants. *Int J Mol Med* 2002; 10: 177–182.
27. Conconi MT, De Coppi P, Bellini S, *et al.* Homologous muscle acellular matrix seeded with autologous myoblasts as a tissue-engineering approach to abdominal wall-defect repair. *Biomaterials* 2005; 26: 2567–2574.
28. Lv FJ, Tuan RS, Cheung KM, *et al.* Concise review: the surface markers and identity of human mesenchymal stem cells. *Stem Cells* 2014; 32: 1408–1419.
29. Amati E, Sella S, Perbellini O, *et al.* Generation of mesenchymal stromal cells from cord blood: evaluation of in vitro quality parameters prior to clinical use. *Stem Cell Res Ther* 2017; 8:14.
30. Ciccocioppo R, Russo ML, Bernardo ME, *et al.* Mesenchymal stromal cell infusions as rescue therapy for corticosteroid-refractory adult autoimmune enteropathy. *Mayo Clin Proc* 2012; 87: 909–914.
31. Galleu A, Riffo-Vasquez Y, Trento C, *et al.* Apoptosis in mesenchymal stromal cells induces in vivo recipient-mediated immunomodulation. *Sci Transl Med* 2017; 9: pii: eaam7828.
32. Uccelli A, Moretta L and Pistoia V. Immunoregulatory function of mesenchymal stem cells. *Eur J Immunol* 2006; 36: 2566–2573.
33. Konala VB, Mamidi MK, Bhonde R, *et al.* The current landscape of the mesenchymal stromal cell secretome: a new paradigm for cell-free regeneration. *Cytotherapy* 2016; 18: 13–24.
34. Amati E, Perbellini O, Rotta G, *et al.* High-throughput immunophenotypic characterization of bone marrow- and cord blood-derived mesenchymal stromal cells reveals common and differentially expressed markers: identification of angiotensin-converting enzyme (CD143) as a marker differentially expressed between adult and perinatal tissue sources. *Stem Cell Res Ther* 2018; 9: 10.
35. Kinzebach S, Dietz L, Klüter H, *et al.* Functional and differential proteomic analyses to identify platelet derived factors affecting ex vivo expansion of mesenchymal stromal cells. *BMC Cell Biol* 2013; 14: 48.
36. Théry C, Witwer KW, Aikawa E, *et al.* Minimal information for studies of extracellular vesicles 2018 (MISEV2018): a position statement of the International Society for Extracellular Vesicles and update of the MISEV2014 guidelines. *J Extracell Vesicles* 2018; 7: 1535750.
37. Dominici M, Le Blanc K, Mueller I, *et al.* Minimal criteria for defining multipotent mesenchymal stromal cells. The International Society for Cellular Therapy position statement. *Cytotherapy* 2006; 8: 315–317.
38. Uccelli A, Moretta L and Pistoia V. Mesenchymal stem cells in health and disease. *Nat Rev Immunol* 2008; 8: 726–736.
39. Merino-Gonzalez C, Zuniga FA, Escudero C, *et al.* Mesenchymal stem cell-derived extracellular vesicles promote angiogenesis: potencial clinical application. *Front Physiol* 2016; 7: 24.
40. Anderson JD, Johansson HJ, Graham CS, *et al.* Comprehensive proteomic analysis of mesenchymal stem cell exosomes reveals modulation of angiogenesis via nuclear factor-kappaB signaling. *Stem Cells* 2016; 34: 601–613.
41. Catry J, Luong-Nguyen M, Arakelian L, *et al.* Circumferential esophageal replacement by a tissue-engineered substitute using mesenchymal stem cells: an experimental study in mini pigs. *Cell Transplant* 2017; 26: 1831–1839.
42. Tan B, Wei RQ, Tan MY, *et al.* Tissue engineered esophagus by mesenchymal stem cell seeding for esophageal repair in a canine model. *J Surg Res* 2013; 182: 40–48.
43. La Francesca S, Aho JM, Barron MR, *et al.* Long-term regeneration and remodeling of the pig esophagus after circumferential resection using a retrievable synthetic scaffold carrying autologous cells. *Sci Rep* 2018; 8: 4123.
44. Park SY, Choi JW, Park JK, *et al.* Tissue-engineered artificial oesophagus patch using three-dimensionally printed polycaprolactone with mesenchymal stem cells: a preliminary report. *Interact Cardiovasc Thorac Surg* 2016; 22: 712–717.
45. Telea Biotech Srl. *Method for preparing an acellular organic tissue*. In: Srl TB, ed. 2007. METODO DI PREPARAZIONE ALLA RIVITALIZZAZIONE DI UN TESSUTO ORGANICO A-CELLULARE E DISPOSITIVO ATTO A REALIZZARE TALE METODO 31/05/2007 Cod. IT0001380537 European extension: EP2164536 B1 (https://worldwide.espacenet.com/publicationDetails/biblio?DB=EPODOC&II=0&ND=3&adjacent=true&locale=en_EP&FT=D&date=20100324&CC=EP&NR=2164536A2&KC=A2)
46. Telea Biotech Srl. *Acellular organic tissue prepared for revitalization and method for*

producing it. 2015. Patent: METODO DI PREPARAZIONE DI UN TESSUTO ORGANICO A-CELLULARE DI ORIGINE UMANA O ANIMALE PER LA RIVITALIZZAZIONE 29/10/2009 Cod. IT1398807 European extension EP2493522 B1 (https://worldwide.espacenet.com/publicationDetails/biblio?DB=EPODOC&II=0&ND=3&adjacent=true&locale=en_EP&FT=D&date=20120905&CC=EP&NR=2493522A1&KC=A1#)

47. Sella S, Adami V, Amati E, *et al.* In-vitro analysis of quantum molecular resonance effects on human mesenchymal stromal cells. *PLoS One* 2018; 13: e0190082.
48. Pozzato G and Vignato G. Teoria della risonanza quantica molecolare nella realizzazione del bisturi elettronico "Vesalius". *Quintessence Int* 2003; 5: 153–155.
49. Dal Maschio M, Canato M and Pigozzo FM. Biophysical effects of high frequency electrical field (4 MHz) on muscle fibers in culture. *Basic Appl Myol* 2009; 19: 49–56.
50. Comite P, Cobianchi L, Avanzini MA, *et al.* Isolation and ex vivo expansion of bone marrow-derived porcine mesenchymal stromal cells: potential for application in an experimental model of solid organ transplantation in large animals. *Transplant Proc* 2010; 42: 1341–1343.
51. Gilpin A and Yang Y. Decellularization strategies for regenerative medicine: from processing techniques to applications. *Biomed Res Int* 2017; 2017: 9831534.
52. Chirica M, Veyrie N, Munoz-Bongrand N, *et al.* Late morbidity after colon interposition for corrosive esophageal injury: risk factors, management, and outcome. A 20-years experience. *Ann Surg* 2010; 252: 271–280.
53. Kanetaka K, Kobayashi S and Eguchi S. Regenerative medicine for the esophagus. *Surg Today* 2018; 48: 739–747.
54. Keane TJ and Badylak SF. The host response to allogeneic and xenogeneic biological scaffold materials. *J Tissue Eng Regen Med* 2015; 9: 504–511.
55. Reames BN and Lin J. Repair of a complex bronchogastric fistula after esophagectomy with biologic mesh. *Ann Thorac Surg* 2013; 95: 1096–1097.
56. Dua KS, Hogan WJ, Aadam AA, *et al.* In-vivo oesophageal regeneration in a human being by use of a non-biological scaffold and extracellular matrix. *Lancet* 2016; 388: 55–61.
57. Nieponice A, Ciotola FF, Nachman F, *et al.* Patch esophagoplasty: esophageal reconstruction using biologic scaffolds. *Ann Thorac Surg* 2014; 97: 283–288.
58. Badylak SF, Hoppo T, Nieponice A, *et al.* Esophageal preservation in five male patients after endoscopic inner-layer circumferential resection in the setting of superficial cancer: a regenerative medicine approach with a biologic scaffold. *Tissue Eng Part A* 2011; 17: 1643–1650.
59. Clough A, Ball J, Smith GS, *et al.* Porcine small intestine submucosa matrix (surgisis) for esophageal perforation. *Ann Thorac Surg* 2011; 91: e15–e16.
60. Paulin D and Li Z. Desmin: a major intermediate filament protein essential for the structural integrity and function of muscle. *Exp Cell Res* 2004; 301: 1–7.